

FgLPMO9A from Fusarium graminearum cleaves xyloglucan independently of the backbone substitution pattern

Nekiunaite, Laura; Petrović, Dejan M.; Westereng, Bjørge; Vaaje-Kolstad, Gustav; Abou Hachem, Maher ; Várnai, Anikó; Eijsink, Vincent G.H.

Published in: F E B S Letters

Link to article, DOI: 10.1002/1873-3468.12385

Publication date: 2016

Document Version Peer reviewed version

Link back to DTU Orbit

Citation (APA):

Nekiunaite, L., Petrović, D. M., Westereng, B., Vaaje-Kolstad, G., Abou Hachem, M., Várnai, A., & Eijsink, V. G. H. (2016). *Fg*LPMO9A from *Fusarium graminearum* cleaves xyloglucan independently of the backbone substitution pattern. *F E B S Letters*, *590*(19), 3346-3356. https://doi.org/10.1002/1873-3468.12385

General rights

Copyright and moral rights for the publications made accessible in the public portal are retained by the authors and/or other copyright owners and it is a condition of accessing publications that users recognise and abide by the legal requirements associated with these rights.

• Users may download and print one copy of any publication from the public portal for the purpose of private study or research.

- You may not further distribute the material or use it for any profit-making activity or commercial gain
- You may freely distribute the URL identifying the publication in the public portal

If you believe that this document breaches copyright please contact us providing details, and we will remove access to the work immediately and investigate your claim.

Received Date : 28-Jun-2016 Revised Date : 11-Aug-2016 Accepted Date : 22-Aug-2016

Article type : Research Letter

*Fg*LPMO9A from *Fusarium graminearum* cleaves xyloglucan independently of the backbone substitution pattern

Laura Nekiunaite¹, Dejan M. Petrović², Bjørge Westereng², Gustav Vaaje-Kolstad², Maher Abou Hachem¹, Anikó Várnai^{2,*}, Vincent G.H. Eijsink²

¹ Enzyme and Protein Chemistry, Department of Systems Biology, Technical University of Denmark, Kongens Lyngby, Denmark

² Department of Chemistry, Biotechnology and Food Science, Norwegian University of Life Sciences, Aas, Norway

* Corresponding author. Department of Chemistry, Biotechnology and Food Science, Norwegian University of Life Sciences, PO Box 5003 (Chr. Magnus Falsens vei 1.), N-1432 Aas, Norway; Phone: +4745174259; Fax: 4764965001 E-mail address: aniko.varnai@nmbu.no.

Abstract

Lytic polysaccharide monooxygenases (LPMOs) are important for the enzymatic conversion of biomass and seem to play a key role in degradation of the plant cell wall. In this study, we characterize an LPMO from the fungal plant pathogen *Fusarium graminearum* (*Fg*LPMO9A) that catalyzes the mixed C1/C4 oxidative cleavage of cellulose and xyloglucan, but is inactive towards other (1,4)-linked β -glucans. Our findings indicate that *Fg*LPMO9A has unprecedented broad specificity on xyloglucan, cleaving any glycosidic bond in the β -glucan main chain, regardless of xylosyl substitutions. Interestingly, we found that when incubated with a mixture of xyloglucan and cellulose, *Fg*LPMO9A efficiently attacks the xyloglucan, whereas cellulose conversion is inhibited. This suggests that removal of hemicellulose may be the true function of this LPMO during biomass conversion.

This article has been accepted for publication and undergone full peer review but has not been through the copyediting, typesetting, pagination and proofreading process, which may lead to differences between this version and the Version of Record. Please cite this article as doi: 10.1002/1873-3468.12385

Keywords: AA9; cellulose; Fusarium graminearum; lytic polysaccharide monooxygenase; xyloglucan.

Abbreviations: AA, auxiliary activity; DP, degree of polymerization; GH, glycoside hydrolase; LPMO, lytic polysaccharide monooxygenase; MALDI-ToF MS, matrix-assisted laser desorption ionization time-of-flight mass spectrometry; PAD, pulsed amperometric detection; PASC, phosphoric acid swollen cellulose; SDS-PAGE, SDS polyacrylamide gel electrophoresis; TXG, tamarind xyloglucan.

INTRODUCTION

Plants have evolved multiple defense mechanisms against microbial pathogens, varying from defense systems triggered by recognition of microbe-associated molecular patterns, to physical barriers, such as the plant cell wall [1,2]. The plant cell wall is the major structural defense barrier against fungal and bacterial pathogens. The composite secondary cell wall consists of cellulose microfibrils embedded in a matrix of hemicellulose and lignin, with cross-linking between the polymers. The primary cell wall, i.e. the thin outer layer of plant cell walls, also contains pectins and structural proteins, which are much less abundant in the secondary walls [3–5]. Many plant pathogenic fungi produce enzymes that allow them to degrade and penetrate this complex plant cell wall barrier [6,7]. *Fusarium graminearum* is a highly destructive pathogen causing *Fusarium* head blight disease on wheat and barley. In addition, this devastating fungus produces mycotoxins, which pose a threat to human and animal health [8]. The genome of *F. graminearum* contains almost 600 predicted carbohydrate-active enzymes (CAZymes). These CAZymes include a variety of glycoside hydrolases (GHs) as well as 18 putative lytic polysaccharide monooxygenases (LPMOs) [9]. *F. graminearum* is an efficient degrader of plant biomass, secreting cell wall degrading enzymes, including cellulases, xylanases, pectinases and LPMOs [10,11].

LPMOs are copper-dependent redox enzymes that oxidatively cleave polysaccharides using molecular oxygen and an electron donor [12–15]. These enzymes are classified as auxiliary activities (AAs) in the Carbohydrate-Active enZyme database, comprising four families, AA9, AA10, AA11, and AA13 (CAZy; http://www.cazy.org) [16]. LPMOs cleave polysaccharides while oxidizing one of the new chain ends at the C1 or C4 position, thus contributing to substrate depolymerization while increasing accessibility of the substrate to conventional GHs [12,15,17,18]. Since their discovery in 2010 [12], LPMOs with preference for various plant polysaccharides, such as cellulose [19,20], xyloglucan and other (1,4)-linked β -glucans [21], starch [22] and xylan [23] have been identified. LPMOs have become an

important ingredient in commercial enzyme cocktails for industrial biomass conversion, such as Cellic CTec2 [24], owing to their synergy with GHs in improving saccharification yields [25,26].

In the present study, we cloned and characterized an AA9 LPMO from *F. graminearum*, hereafter referred to as *Fg*LPMO9A, which is the first *F. graminearum* LPMO to be characterized. We studied the action of *Fg*LPMO9A on various plant polysaccharides including cellulose and xyloglucan as well as mixtures of these two. We show that *Fg*LPMO9A possesses unprecedented broad specificity when acting on xyloglucan and we speculate that hemicellulose degradation may be the enzyme's true biological function.

MATERIALS AND METHODS

Cloning and expression of the F. graminearum LPMO

The gene encoding *Fg*LPMO9A [UniProt: 11REU9], including its native signal sequence, was codon optimized for *Pichia pastoris* (GenScript, NJ, USA). The synthetic gene was inserted into the pPink-GAP vector, which was then transformed into *P. pastoris* PichiaPink^M Strain 4 cells (Invitrogen, CA, USA), as described earlier [27]. Transformants were screened for protein production in BMGY medium (containing 1% (v/v) glycerol).

The best-producing transformant was pre-grown in 20 ml of BMGY medium (containing 1% (v/v) glycerol) in a 100-ml shake flask at 29 °C and 200 rpm for 16 hours. This pre-culture was used to inoculate 0.5 l BMGY medium (containing 1% (v/v) glycerol) in a 2-l baffled shake flask. After 24 hours of incubation at 29 °C and 200 rpm, the medium was supplemented with 1% (v/v) glycerol. After a total incubation time of 48 hours, the cells were harvested by centrifugation at 7,000 × *g* for 15 min. The supernatant was filtered through a 0.2-µm polyethersulfone membrane (Millipore, MA, USA), dialyzed against 50 mM Bis-Tris buffer (pH 6.5), and concentrated to 50 ml with a VivaFlow 50 tangential crossflow concentrator (MWCO 10 kDa, Sartorius Stedim Biotech, Germany).

Purification and Cu(II) saturation of the enzyme

*Fg*LPMO9A was purified using a two-step purification protocol, starting with hydrophobic interaction chromatography (HIC) followed by size exclusion chromatography (SEC). The concentrated culture supernatant was prepared for HIC by slow addition of solid ammonium sulfate to 2.03 M final concentration, at 20 °C, followed by centrifugation (15,000 × *g*, 15 min, 4 °C). The sample was loaded

onto a 5-ml HiTrap Phenyl FF column (GE Healthcare, Sweden) equilibrated with 50 mM Bis-Tris buffer (pH 6.5), containing 2.03 M ammonium sulfate. Proteins bound to the column were eluted using a 25-ml linear gradient from 2.03 M to 0 M ammonium sulfate in 50 mM Bis-Tris buffer (pH 6.5). Collected fractions were analyzed by sodium dodecyl sulfate–polyacrylamide gel electrophoresis (SDS–PAGE), and the fractions containing *Fg*LPMO9A were pooled and concentrated using Amicon Ultra centrifugal filters (MWCO 10 kDa, Millipore). The sample was saturated with Cu(II) by incubating the enzyme with an excess of CuSO₄ (at 3:1 molar ratio of copper:enzyme) for 30 min at room temperature as described previously [28]. Subsequently, the sample was loaded onto a HiLoad 16/60 Superdex 75 size exclusion column (GE Healthcare) in 50 mM Bis-Tris buffer (pH 6.5), using a flow rate of 1.0 ml/min. Fractions containing pure protein were identified using SDS-PAGE and subsequently pooled and concentrated using Amicon Ultra centrations were determined using the Bradford assay (Bio-Rad).

NcLPMO9C from *Neurospora crassa* [UniProt:Q7SHI8] was expressed in *P. pastoris* X-33 and purified as described previously [29].

Substrates used for enzyme specificity analysis

The following substrates were used for exploring enzymatic activities of *Fg*LPMO9A: phosphoric acid swollen cellulose (PASC) prepared from Avicel as described by Wood [30]; xyloglucan (XG) from tamarind seed; xyloglucan-heptamer (XG7 or XXXG, where X stands for glucose, G, substituted at the C6 position with xylose); xyloglucan oligomers (XG-oligomers) derived from tamarind xyloglucan mainly containing XXXGXXXG, with 0–3 galactose substitutions (L stands for X where the xylose is substituted at the C2 position with a galactose; it is not known which X is galactosylated); a reduced 14-mer (XG14^{OH}) mainly containing XXXGXXXG^{OH} and variants containing one or more L instead of X (the reducing end D-glucose is reduced to a D-glucitol). *Fg*LPMO9A was also screened against cello-oligosaccharides (Glc₃₋₆), birchwood xylan, wheat arabinoxylan, konjac glucomannan, ivory nut mannan, barley β-glucan, lichenan from Icelandic moss, starch, and deacetylated galactoglucomannan from Norway spruce. Birchwood xylan was purchased from Sigma-Aldrich (MO, USA), starch was purchased from Merck (Darmstadt, Germany). All other substrates were purchased from Megazyme (Ireland).

Enzyme activity assays

Reaction mixtures with single substrates contained 2 mg/ml substrate, while the reactions with substrate mixtures contained 2 mg/ml PASC and 2 mg/ml of the other polysaccharide. Reaction mixtures

additionally contained 2 μ M *Fg*LPMO9A or *Nc*LPMO9C and 1 mM ascorbic acid in 20 mM Bis-Tris buffer (pH 6.5) in a total volume of 100 μ l, in 2-ml Eppendorf tubes. Samples were incubated at 15 or 45 °C in an Eppendorf Thermomixer (Eppendorf AG, Germany) with shaking at 900 rpm. After incubation, the reaction mixtures were placed on ice and the reactions were immediately stopped by boiling for 10 min, before separating soluble and insoluble fractions using a 96-well filter plate (Millipore) operated by a Millipore vacuum manifold. Control reactions were performed using identical conditions, but in the absence of ascorbic acid.

Analysis of enzyme products

Products generated by the LPMOs were analyzed using MALDI-ToF mass spectrometry (MS) and high-performance anion exchange chromatography (HPAEC) as follows. MALDI-ToF MS analysis was performed with an Ultraflex MALDI-ToF/ToF instrument (Bruker Daltonics, Germany) equipped with a Nitrogen 337 nm laser beam as described by Vaaje-Kolstad et al. [12]. The instrument was operated in positive acquisition mode and controlled by the FlexControl 3.3 software package. The data were processed with mMass software [31]. Baseline correction and Gaussian smoothing (window size 0.3 m/z) were applied to all spectra. Prior to MALDI-ToF MS analysis, the samples were saturated with sodium by mixing 5 µl sample with 5 µl 50 mM sodium acetate, followed by 30 min incubation, sample spotting and drying.

HPAEC analysis was performed on a Dionex ICS-5000 system (Dionex, CA, USA) equipped with pulsed amperometric detection (PAD) and a CarboPac PA1 analytical column (2×250 mm) with a CarboPac PA1 guard column (2×50 mm). The system was operated at a flow rate of 0.25 ml/min and kept at 30 °C while running a 75-min stepwise gradient as described by Agger et al. [21]. The data were collected and analyzed using Chromeleon 7.0 (Dionex).

RESULTS

Heterologous expression of FgLPM09A from F. graminearum

Recombinant FgLPMO9A was successfully expressed by growing P. pastoris in BMGY medium for 48 hours. The enzyme was purified in two chromatographic steps to \approx 95% purity, as confirmed by SDS-PAGE (see Fig. S1). The protein band representing FgLPMO9A appears as a broad band in the 60–70 kDa range, whereas the theoretical molecular mass calculated from the amino acid sequence is 32 kDa. The observed mass difference is likely due to O- and/or N-glycosylation, which are predicted (using the

NetOGlyc and NetNGlyc servers available at http://www.cbs.dtu.dk/services) to possibly occur at Ser/Thr 234, 235, 238, 240, 241, 243, 245, 247, 249, 251, 257, 262, 287, 292 and Asn211, respectively. Such mass differences are not uncommon although in the present case the difference is rather large, possibly due to a large number of O-glycosylations in the C-terminal region of low complexity and unknown function (residues 226-314). Notably, these putative *O*-glycosylations are likely to affect the substrate-binding surface of the LPMO. Sequence alignments and structural modelling indicated that the only potential N-glycosylation site (Asn211) is located far away from the catalytic center and that the side chain of this residue points away from the substrate-binding surface. Attempts to deglycosylate the enzyme by treatment with PNGase F from *Flavobacterium meningosepticum* (New England Biolabs, Ipswich, MA) or α -mannosidase from *Canavalia ensiformis* (Sigma-Aldrich) were not successful, although a small shift in electrophoretic mobility was observed with the latter enzyme (results not shown).

Substrate specificity

In order to determine substrate specificity, *Fg*LPMO9A was incubated with a wide range of oligoand polysaccharides in the presence of an electron donor. Studies with insoluble substrates showed that the enzyme is capable of cleaving cellulose (Fig. 1), but not chitin (results not shown). No activity was detected towards shorter cellooligosaccharides (Glc₃₋₆; results not shown). Among the tested hemicelluloses, *Fg*LPMO9A was active on tamarind xyloglucan and longer xyloglucan oligosaccharides (see below for details). No activity was observed towards the xyloglucan-heptamer (XXXG), birchwood xylan, wheat arabinoxylan, konjac glucomannan, ivory nut mannan, β -glucan from barley, lichenan from Icelandic moss, starch, and spruce galactoglucomannan (data not shown).

Activity on amorphous cellulose (PASC)

When using PASC as a substrate, HPAEC analysis of the products generated by *Fg*LPMO9A showed native as well as C1- and C4-oxidized cellooligosaccharides (Fig. 1A). In the absence of an electron donor, no LPMO activity was detected. Oxidative cleavage of cellulose and the C1/C4 mixed oxidation pattern were confirmed by MALDI-ToF MS analysis of the released products (Fig. 1B–C). Notably, both types of oxidized products may occur in the non-hydrated and the hydrated form, the latter being a gemdiol for C4-oxidized products and an aldonic acid for C1-oxidized products. For the C4-oxidized compounds, the non-hydrated ketoaldose form is favored (m/z 1335.7, for DP 8). On the other hand, C1-oxidized compounds largely occur as the hydrated aldonic acid form (m/z 1353.6 for DP 8), which at neutral conditions forms a diagnostic sodium salt (m/z 1375.5 for DP 8). Other species visible in Fig. 1C are the native oligomer (m/z 1337.7), a double-oxidized oligomer with one hydration (m/z 1351.6), and a

double-oxidized oligomer with two hydrations (m/z 1369.6). The appearance of native oligosaccharides and double-oxidized oligosaccharides confirms C1/C4 mixed oxidation. All product clusters, ranging in DP from 5 to 10 (Fig. 1B), showed adduct distributions similar to that shown for the DP 8 cluster in Fig. 1C.

Activity on tamarind xyloglucan

During the course of this study, we noted that the activity of *Fg*LPMO9A was considerably higher at 15 °C compared to 45 °C; hence reactions with TXG were carried out at both temperatures. *Fg*LPMO9A was capable of cleaving tamarind xyloglucan (TXG), and HPAEC analysis (Fig. 2) revealed a more complex product profile compared to the product profile generated by *Nc*LPMO9C ([21]; see below). *Fg*LPMO9A produced a mixture of oligosaccharides, some of which corresponded to the native xyloglucan heptasaccharide (XXXG), eluting at 26 min. Some species eluted before XXXG, which are likely to be shorter native fragments, such as XXX, eluting at 22 min (see [21]). The elution profile in the 50-55 min range is similar to the profile previously published for *Nc*LPMO9C [21]. In addition, a broad range of products appears at 26-50 min that has not been observed before, not for *Nc*LPMO9C, nor for the other xyloglucan-active LPMOS described so far, *Pa*LPMO9H and *Tt*LPMO9E [21,32,33]. Although some of these peaks may correspond to longer native XG oligomers (see black line in Fig. 2), most of the products released from TXG remain unidentified due to the heterogeneity of the substrate and lack of standards.

Analysis of the reaction products with MALDI-ToF MS revealed that *Fg*LPMO9A indeed produces a much wider range of native and oxidized xyloglucan-oligosaccharides (Fig. 3A), compared to *Nc*LPMO9C (Fig. 3B). Both enzymes released a cluster of $\text{Hex}_n\text{Pen}_3^{\text{ox}}$ products with *m/z* 1083.7 (n=4), *m/z* 1245.5 (n=5), and *m/z* 1407.5 (n=6) and a cluster of $\text{Hex}_n\text{Pen}_6^{\text{ox}}$ products with *m/z* 2452.1 (n=10), *m/z* 2614.1 (n=11), and *m/z* 2776.2 (n=12), where Hex stands for a hexose (glucose or galactose, 162.14 Da) and Pen for a pentose (xylose, 132.11 Da). Only *Fg*LPMO9A released a wide variety of additional products where the number of pentoses does not equal a multitude of 3. As an example, Fig. 3C shows signals for Hex₇Pen₄^{ox}, showing a double oxidized species (*m/z* = 1699.5), a single oxidized species (*m/z* = 1701.5), the native species (*m/z* = 1703.6), and hydrated single (*m/z* = 1719.6) and double (*m/z* = 1717.5) oxidized species. Taken together, the data in Figs. 3A-C show that while *Nc*LPMO9C only cleaves at the unsubstituted glucose unit and exclusively oxidizes C4 [21], *Fg*LPMO9A oxidizes both C1 and C4 and cleaves TXG at any position in the β -glucan backbone, i.e. also between two substituted units (Fig. 3D).

Activity on mixtures of hemicelluloses and PASC

It has previously been shown that certain LPMOs can cleave xylan, only if the xylan is complexed with cellulose [23]. In order to gain further insight into the potential role of *Fg*LPMO9A in plant cell wall degradation, we mixed cellulose (PASC) with different hemicelluloses and treated the resulting polysaccharide mixtures with *Fg*LPMO9A, in the presence or absence of ascorbic acid as electron donor. Mixing PASC with birchwood xylan or ivory nut mannan reduced PASC conversion, while mixing with konjac glucomannan completely inhibited activity on PASC. We were not able to detect cleavage of these three hemicelluloses (data not shown). Upon mixing TXG and PASC, activity on PASC was greatly reduced, whereas the activity on TXG was hardly affected (Fig. 2; note the lack of native cello-oligomers in the red chromatograms, relative to the green chromatograms).

It is conceivable that mixing TXG with PASC leads to complexation where the hemicellulose forms a physical barrier on the surface of the cellulose. To investigate this further, we carried out studies with a cellulose-active LPMO that is inactive towards xyloglucan. These studies showed that the activity of the cellulose-active LPMO was inhibited by adding TXG to the PASC and that this inhibition could be relieved by adding an enzyme degrading TXG (for details, see Fig. S2 and supporting discussion).

Activity on a reduced xyloglucan-oligosaccharide (XG14)

To gain a deeper understanding of the *Fg*LPMO9A activity towards TXG, we studied the degradation products generated by the enzyme when incubated with the reduced form of a relatively pure xyloglucan oligosaccharide with DP14 (XG14^{OH}). The sequence of this oligomer is XXXGXXG^{OH}, where G^{OH} represents a D-glucitol, reduced glucose, at the reducing end, leading to an *m/z* shift of +2 Da compared to a native species. The product profile was analyzed using HPAEC and MALDI-ToF MS (Fig. 4). Only in the presence of ascorbic acid, *Fg*LPMO9A generated a variety of products, including the native XXXG peak eluting at 26 min and several additional compounds eluting before XXXG, such as the native XXX at 22 min. These latter compounds also appeared in the chromatograms obtained upon degradation of TXG by *Fg*LPMO9A (Fig. 2) and are likely to be shorter native fragments. In addition, some of these compounds may be reduced oligosaccharides [21]. At the same time, several product species eluting after the substrate, at 44-48 min and at 56-64 min, were visible similar to products generated by *Nc*LPMO9C from this same substrate [21].

Oxidative cleavage of XG14^{OH} by *Fg*LPMO9A was confirmed by analysis of the products with MALDI-ToF MS (Fig. 4B). A single cleavage of XG14^{OH} with C1-oxidation generates two products that differ with

 $\Delta m/z \pm 2$ from the native ones: the non-reducing end product carrying the C1-oxidation ($\Delta m/z=-2$) and the reducing end product carrying the reduced glucose at the "reducing" end ($\Delta m/z$ =+2). On the other hand, a single cleavage with C4-oxidation generates two products with masses identical to those of native species ($\Delta m/z=0$): the non-reducing end product is a native oligosaccharide and the reducing end product carries a keto-group from the C4-oxidation ($\Delta m/z$ =-2) and the reduced D-glucitol at the "reducing end" ($\Delta m/z$ =+2), (Fig. 4C). The mass spectrum shows a wide range of xyloglucan oligosaccharides with masses corresponding to native species or differing from that with $\Delta m/z=\pm 2$, showing that both C1 and C4 oxidation occurred and that the enzyme can cleave the substrate at several positions. The only two C1-oxidized products detected were $\text{Hex}_3\text{Pen}_3^{\text{ox}}$ (m/z = 921.5; $\Delta m/z$ =-2) and Hex₄Pen₃^{ox} (m/z = 1083.7; $\Delta m/z=-2$), which are indicative of C1 oxidation at the non-substituted glucose, perhaps only on the non-reducing side of this glucose (due to varying galactosylation, both Hex₃Pen₃^{ox} and Hex₄Pen₃^{ox} could be products). The occurrence of a wide variety of products with a number of pentoses not equaling a multitude of 3 shows that cleavage between two substituted units occurred. The fact that these products emerged both as reduced species ($\Delta m/z=+2$) and native species ($\Delta m/z=0$) shows that both C1- and C4-oxidation occur during cleavage in between substituted units (e.g. m/z 1115.6 and 1117.6 for Hex_5Pen_2 , or m/z 1541.8 and 1543.7 for Hex_6Pen_4).

DISCUSSION

The discovery of LPMOs has been a significant breakthrough in understanding how plant biomass is degraded in nature, and has also had major technological implications, as illustrated by the fact that, today, these enzymes are important components of enzyme cocktails for industrial biomass conversion [34]. LPMOs are produced not only by saprophytic fungi but also by plant pathogens, suggesting a putative role of these enzymes in plant cell wall degradation during pathogenesis [10]. *F. graminarum* displays both a saprophytic and a pathogenic lifestyle and to what extend *Fg*LPMO9A plays a role in each of these is not yet known. Notably, it has been shown that most of the putative LPMOs encoded in the genome of *F. graminearum*, including *Fg*LPMO9A, are upregulated during infection of barley and wheat [35]. Although to date the CAZy database harbors more than 400 fungal LPMOs, only about 20 of these enzymes have been characterized, and these are all from saprophytic fungi. To our knowledge, *Fg*LPMO9A is the first LPMO from a plant pathogen to be characterized.

*Fg*LPMO9A has mixed oxidative regioselectivity, oxidizing both C1 and C4 in insoluble (cellulose) and soluble (xyloglucan) substrates. The enzyme produces relatively large amounts of native cello- and xyloglucan-oligosaccharides (Figs. 1–3). Native products are commonly observed for mixed activity LPMOs, and could emerge when a single polysaccharide chain is cleaved twice, once with C1 and once with C4 oxidation, with the C1 oxidation happening upstream of the C4 oxidation. Notably, native products are also commonly observed with HPAEC analysis for strictly C4 oxidizing LPMOs, as C4-oxidized products are converted to native cello-oligomers after losing the 4-ketoglucose at the non-reducing end (upstream end), promoted by the conditions of standard HPAEC analysis, which has recently been shown [36]. Hence, some of the native oligosaccharides seen in the HPAEC profile are likely degradation products of the corresponding C4-oxidized compounds. Control reactions, where ascorbic acid was excluded from the reaction, showed no formation of oxidized or native xyloglucan- or cello-oligomers, verifying that the *Fg*LPMO9A preparation was free of contaminating background endo- β -1,4-glucanase activity.

So far, only four LPMOs have been reported to cleave xyloglucan, namely *NcL*PMO9C from *Neurospora crassa*, *PaL*PMO9H from *Podospora anserina*, AN3046 LPMO from *Aspergillus nidulans* and *TtL*PMO9E from *Thielavia terrestris*; and the cleavage pattern of *NcL*PMO9C and *PaL*PMO9H has been reported [21,32,33,37]. Both enzymes cleave xyloglucan exclusively adjacent to the unsubstituted glucosyl unit, with *NcL*PMO9C only yielding C4-oxidized products, whereas *PaL*PMO9H yields a mixture of C1- and C4-oxidized products with the latter being dominant [32]. Considering the oxidative mechanism, *FgL*PMO9A is more similar to *PaL*PMO9H since it oxidizes both C1 and C4. However, *FgL*PMO9A is fundamentally different from both enzymes described above, since *FgL*PMO9A is not restricted to cleaving by the unsubstituted glucosyl, thereby generating a broader product spectrum. The lack of activity on cellohexaose further separates *FgL*PMO9A from *NcL*PMO9C and *PaL*PMO9H, the two well-characterized xyloglucan-active LPMOs, and indicates that the catalytic site of *FgL*PMO9A needs to accommodate a β -1,4-glucan chain with more than six glucose residues for catalysis to happen.

Interestingly, the XG-cleaving properties of *Fg*LPMO9A are not commonly found amongst XG-active enzymes, as the majority of GHs cleaving this polymer are selective for non-substituted backbone glucose residues. The only GHs known to cleave XG between substituted backbone residues are found in the GH74 family [38,39]. Thus, our findings provide a new activity to the XG enzymatic toolbox. The *F. graminearum* genome only contains one GH74 enzyme, which has not yet been characterized and thus has an unknown function (the GH74 family also harbors enzymes with endoglucanase and exo-

xyloglucanase activity). It may be that *Fg*LPMO9A plays a crucial role in the XG degradative machinery of the fungus by providing the ability to cleave between substituted backbone residues.

The effect of temperature on *Fg*LPMO9A activity is remarkable and has several potential explanations. Control experiments showed that the enzyme is thermally stable under the conditions used (see Fig. S3 and supporting discussion), excluding temperature-induced denaturation as an explanation. In this qualitative study of the activity of *Fg*LPMO9A, we routinely used 16-hour incubation times. A closer examination of product formation over time (Fig. S4) revealed that enzyme activity ceases already after 1–4 hours. Higher incubation temperatures lead to faster initial rates but more rapid inactivation of the enzyme, the net effect being that incubation at the lower temperature gives higher final product yields. Enzyme inactivation is often observed in LPMO reactions but has hardly been discussed and remains unexplained. Inactivation could be due to the production of H₂O₂ [29] and more powerful oxidative species (such as hydroxyl radicals) that may damage the LPMO molecule. A further discussion of this issue is beyond the scope of this paper, but the present data show that this issue deserves more attention.

*Fg*LPMO9A did not show detectable activity on xylan, arabinoxylan, glucomannan, mannan, βglucan, or lichenan. Mixing PASC with several hemicelluloses did not reveal hemicellulolytic activities beyond activity on xyloglucan but did show inhibition of activity on PASC, likely because hemicellulose-PASC associations shield the cellulose. This observation was explored further for xyloglucan, which is thought to associate with cellulose to form load-bearing networks in plant primary cell walls [3,40,41]. Interestingly, when using a mixture of xyloglucan and cellulose as substrate, the activity of *Fg*LPMO9A on xyloglucan was maintained, whereas activity on cellulose was strongly reduced. Control experiments with a cellulose-active LPMO that is not active on xyloglucan (see Supporting information) showed that cellulose degradation is inhibited by the addition of xyloglucan and that such inhibition may be relieved by also adding a xyloglucanase. All in all, these data suggest that xyloglucan shields cellulose from being degraded by *Fg*LPMO9A and that one natural function of this LPMO could be to make cellulose accessible.

LPMOs are thought to have a big impact on the depolymerization of organic matter in nature [42]. It is conceivable that *Fg*LPMO9A, with its unique ability to randomly cleave xyloglucan, contributes to overcoming the plant cell wall barrier by removing hemicellulose and by making other polymers such as cellulose more accessible for enzymatic degradation.

SUPPORTING INFORMATION

Additional supporting information, including Figs. S1–S4 may be found in the online version of this article at the publisher's web site.

ACKNOWLEDGEMENTS

This work was funded in part by the Research Council of Norway through grants 214613 & 243663. We thank Roland Ludwig and colleagues for the clone producing *Nc*LPMO9C. LN was funded by the Novo Nordisk foundation with a "Biotechnology-based Synthesis and Production" grant (NNF12OC0000769).

REFERENCES

- 1. Grennan AK (2006) Plant response to bacterial pathogens. Overlap between innate and gene-forgene defense response. *Plant Physiol* **142**, 809-811.
- Ponce de León I, Montesano M (2013) Activation of defense mechanisms against pathogens in mosses and flowering plants. *Int J Mol Sci* 14, 3178-3200.
- Carpita NC, Gibeaut DM (1993) Structural models of primary cell walls in flowering plants: consistency of molecular structure with the physical properties of the walls during growth. *Plant J* 3, 1-30.
- 4. Cosgrove DJ (2005) Growth of the plant cell wall. Nat Rev Mol Cell Biol 6, 850-861.
- 5. Doblin MS, Pettolino F, Bacic A (2010) Plant cell walls: the skeleton of the plant world. *Funct Plant Biol* **37**, 357-381.
- Laluk K, Mengiste T (2010) Necrotroph attacks on plants: wanton destruction or covert extortion? Arabidopsis Book 8, e0136.
- 7. Kubicek CP, Starr TL, Glass NL (2014) Plant cell wall-degrading enzymes and their secretion in plantpathogenic fungi. *Annu Rev Phytopathol* **52**, 427-451.
- 8. Goswami RS, Kistler HC (2004) Heading for disaster: *Fusarium graminearum* on cereal crops. *Mol Plant Pathol* **5**, 515-525.
- King R, Urban M, Hammond-Kosack MCU, Hassani-Pak K, Hammond-Kosack KE (2015) The completed genome sequence of the pathogenic ascomycete fungus *Fusarium graminearum*. *BMC Genomics* 16, 544.

- Paper JM, Scott-Craig JS, Adhikari ND, Cuomo CA, Walton JD (2007) Comparative proteomics of extracellular proteins *in vitro* and *in planta* from the pathogenic fungus *Fusarium graminearum*. *Proteomics* 7, 3171-3183.
- 11. Debeire P, Delalande F, Habrylo O, Jeltsch JM, Van Dorsselaer A, Phalip V (2014) Enzymatic cocktails produced by *Fusarium graminearum* under submerged fermentation using different lignocellulosic biomasses. *FEMS Microbiol Lett* **355**, 116-123.
- 12. Vaaje-Kolstad G, Westereng B, Horn SJ, Liu Z, Zhai H, Sørlie M, Eijsink VGH (2010) An oxidative enzyme boosting the enzymatic conversion of recalcitrant polysaccharides. *Science* **330**, 219-222.
- 13. Hemsworth GR, Davies GJ, Walton PH (2013) Recent insights into copper-containing lytic polysaccharide mono-oxygenases. *Curr Opin Struct Biol* **23**, 660-668.
- Kjaergaard CH, Qayyum MF, Wong SD, Xu F, Hemsworth GR, Walton DJ, Young NA, Davies GJ, Walton PH, Johansen KS, *et al.* (2014) Spectroscopic and computational insight into the activation of O2 by the mononuclear Cu center in polysaccharide monooxygenases. *Proc Natl Acad Sci U S A* 111, 8797-8802.
- 15. Beeson WT, Phillips CM, Cate JHD, Marletta MA (2012) Oxidative cleavage of cellulose by fungal copper-dependent polysaccharide monooxygenases. *J Am Chem Soc* **134**, 890-892.
- 16. Levasseur A, Drula E, Lombard V, Coutinho PM, Henrissat B (2013) Expansion of the enzymatic repertoire of the CAZy database to integrate auxiliary redox enzymes. *Biotechnol Biofuels* **6**, 41.
- 17. Vu VV, Beeson WT, Phillips CM, Cate JHD, Marletta MA (2014) Determinants of regioselective hydroxylation in the fungal polysaccharide monooxygenases. *J Am Chem Soc* **136**, 562-565.
- Isaksen T, Westereng B, Aachmann FL, Agger JW, Kracher D, Kittl R, Ludwig R, Haltrich D, Eijsink
 VGH, Horn SJ (2014) A C4-oxidizing lytic polysaccharide monooxygenase cleaving both cellulose and cello-oligosaccharides. *J Biol Chem* 289, 2632-2642.
- Quinlan RJ, Sweeney MD, Lo Leggio L, Otten H, Poulsen JCN, Johansen KS, Krogh KBRM, Jørgensen CI, Tovborg M, Anthonsen A, *et al.* (2011) Insights into the oxidative degradation of cellulose by a copper metalloenzyme that exploits biomass components. *Proc Natl Acad Sci U S A* 108, 15079-15084.
- Forsberg Z, Vaaje-Kolstad G, Westereng B, Bunæs AC, Stenstrøm Y, Mackenzie A, Sørlie M, Horn SJ, Eijsink VGH (2011) Cleavage of cellulose by a CBM33 protein. *Protein Sci* 20, 1479-1483.
- 21. Agger JW, Isaksen T, Várnai A, Vidal-Melgosa S, Willats WGT, Ludwig R, Horn SJ, Eijsink VGH,

Westereng B (2014) Discovery of LPMO activity on hemicelluloses shows the importance of oxidative processes in plant cell wall degradation. *Proc Natl Acad Sci U S A* **111**, 6287-6292.

- 22. Vu VV, Beeson WT, Span EA, Farquhar ER, Marletta MA (2014) A family of starch-active polysaccharide monooxygenases. *Proc Natl Acad Sci U S A* **111**, 13822-13827.
- Frommhagen M, Sforza S, Westphal AH, Visser J, Hinz SWA, Koetsier MJ, van Berkel WJH, Gruppen H, Kabel MA (2015) Discovery of the combined oxidative cleavage of plant xylan and cellulose by a new fungal polysaccharide monooxygenase. *Biotechnol Biofuels* 8, 101.
- 24. Cannella D, Jørgensen H (2014) Do new cellulolytic enzyme preparations affect the industrial strategies for high solids lignocellulosic ethanol production? *Biotechnol Bioeng* **111**, 59-68.
- Müller G, Várnai A, Johansen KS, Eijsink VGH, Horn SJ (2015) Harnessing the potential of LPMOcontaining cellulase cocktails poses new demands on processing conditions. *Biotechnol Biofuels* 8, 187.
- Hu J, Chandra R, Arantes V, Gourlay K, van Dyk JS, Saddler JN (2015) The addition of accessory enzymes enhances the hydrolytic performance of cellulase enzymes at high solid loadings. *Bioresour Technol* 186, 149-153.
- 27. Várnai A, Tang C, Bengtsson O, Atterton A, Mathiesen G, Eijsink VGH (2014) Expression of endoglucanases in *Pichia pastoris* under control of the GAP promoter. *Microb Cell Fact* **13**, 57.
- 28. Loose JSM, Forsberg Z, Fraaije MW, Eijsink VGH, Vaaje-Kolstad G (2014) A rapid quantitative activity assay shows that the *Vibrio cholerae* colonization factor GbpA is an active lytic polysaccharide monooxygenase. *FEBS Lett* **588**, 3435-3440.
- 29. Kittl R, Kracher D, Burgstaller D, Haltrich D, Ludwig R (2012) Production of four *Neurospora crassa* lytic polysaccharide monooxygenases in *Pichia pastoris* monitored by a fluorimetric assay.
 Biotechnol Biofuels 5, 79.
- Wood TM (1988) Preparation of crystalline, amorphous, and dyed cellulase substrates. *Methods Enzymol* 160, 19-25.
- 31. Strohalm M, Kavan D, Novák P, Volný M, Havlícek V (2010) mMass 3: a cross-platform software environment for precise analysis of mass spectrometric data. *Anal Chem* **82**, 4648-4651.
- Bennati-Granier C, Garajova S, Champion C, Grisel S, Haon M, Zhou S, Fanuel M, Ropartz D, Rogniaux H, Gimbert I, *et al.* (2015) Substrate specificity and regioselectivity of fungal AA9 lytic polysaccharide monooxygenases secreted by *Podospora anserina*. *Biotechnol Biofuels* 8, 90.

- Cannella D, Möllers KB, Frigaard NU, Jensen PE, Bjerrum MJ, Johansen KS, Felby C (2016) Lightdriven oxidation of polysaccharides by photosynthetic pigments and a metalloenzyme. *Nat Comm* 7, 11134.
- Johansen KS (2016) Discovery and industrial applications of lytic polysaccharide monooxygenases. Biochem Soc Trans 44, 143-149.
- 35. Zhao Z, Liu H, Wang C, Xu JR (2014) Comparative analysis of fungal genomes reveals different plant cell wall degrading capacity in fungi. *BMC Genomics* **15**, 6.
- 36. Westereng B, Arntzen MØ, Aachmann FL, Várnai A, Eijsink VG, Agger JW (2016) Simultaneous analysis of C1 and C4 oxidized oligosaccharides, the products of lytic polysaccharide monooxygenases (LPMOs) acting on cellulose. *J Chromatogr A* **1445**, 46-54.
- 37. Jagadeeswaran G, Gainey L, Prade R, Mort AJ (2016) A family of AA9 lytic polysaccharide monooxygenases in *Aspergillus nidulans* is differentially regulated by multiple substrates and at least one is active on cellulose and xyloglucan. *Appl Microbiol Biotechnol* **100**, 4535-4547.
- Desmet T, Cantaert T, Gualfetti P, Nerinckx W, Gross L, Mitchinson C, Piens K (2007) An investigation of the substrate specificity of the xyloglucanase Cel74A from *Hypocrea jecorina*. *FEBS J* 274, 356-363.
- 39. Feng T, Yan KP, Mikkelsen MD, Meyer AS, Schols HA, Westereng B, Mikkelsen JD (2014) Characterisation of a novel endo-xyloglucanase (XcXGHA) from *Xanthomonas* that accommodates a xylosyl-substituted glucose at subsite -1. *Appl Microbiol Biotechnol* **98**, 9667-9679.
- 40. Park YB, Cosgrove DJ (2015) Xyloglucan and its interactions with other components of the growing cell wall. *Plant Cell Physiol* **56**, 180-194.
- **41.** Burton R a, Gidley MJ, Fincher GB (2010) Heterogeneity in the chemistry, structure and function of plant cell walls. *Nat Chem Biol* **6**, 724-732.
- 42. Hori C, Gaskell J, Igarashi K, Samejima M, Hibbett D, Henrissat B, Cullen D (2013) Genomewide analysis of polysaccharides degrading enzymes in 11 white- and brown-rot Polyporales provides insight into mechanisms of wood decay. *Mycologia* **105**, 1412-1427.
- Varki A, Cummings RD, Aebi M, Packer NH, Seeberger PH, Esko JD, Stanley P, Hart G, Darvill A, Kinoshita T, *et al.* (2015) Symbol nomenclature for graphical representations of glycans. *Glycobiology* 25, 1323-1324.

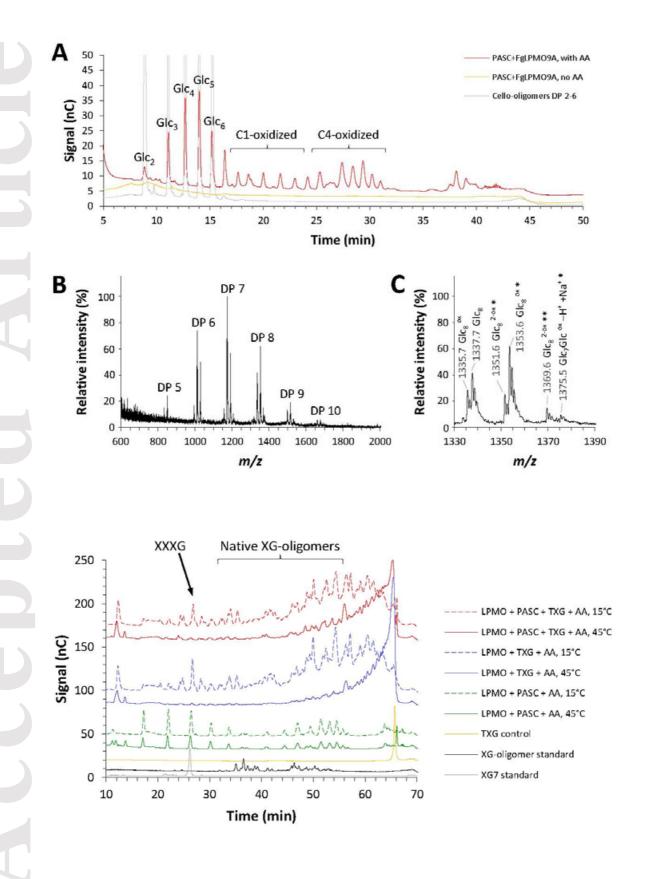
FIGURE LEGENDS

Figure 1. Reaction products generated by *Fg*LPMO9A from PASC. **(A)** HPAEC-PAD profiles of reaction mixtures containing *Fg*LPMO9A and PASC, with (red line) and without (yellow line) ascorbic acid; the grey line shows cello-oligosaccharide standards with DP 2-6. The produced oxidized and native cello-oligosaccharides are labeled in the figure and annotations are based on previous work [17,18]. **(B)** MALDI-ToF MS spectrum of oligosaccharides released from PASC by *Fg*LPMO9A, ranging from DP 5-10, after Na⁺-saturation. **(C)** Close-up of the DP 8 cluster showing the sodium adduct of native and oxidized products; single or double oxidation is denoted with "ox and 2-ox"; single or double hydration is indicated by * or **. See text for a discussion of the various peaks.

Figure 2. HPAEC-PAD chromatograms showing products obtained after *Fg*LPMO9A action on tamarind xyloglucan (TXG, blue), PASC (green) or 1:1 TXG-PASC mixtures (red). Samples were incubated at 15 °C (dashed lines) or 45 °C (solid lines) with ascorbic acid (AA) for 16 hours. In addition, chromatograms for a xyloglucan-oligosaccharide standard (black line), a xyloglucan heptamer (XXXG) standard (grey line) and TXG (yellow line) are shown. Control reactions showed that neither native nor oxidized xyloglucan oligosaccharides were generated by *Fg*LPMO9A in the absence of an electron donor.

Figure 3. Reaction products generated from tamarind xyloglucan (TXG). **(A,B)** MALDI-ToF MS spectra showing product profiles generated from TXG by **(A)** *Fg*LPMO9A and **(B)** *Nc*LPMO9C with oxidized product peak annotations. Note the much more complex product profile obtained with *Fg*LPMO9A. **(C)** Close-up of the Hex₇Pen₄ cluster showing the sodium adduct of native and oxidized products; single or double oxidation is denoted with "ox and 2-ox"; hydration is labeled with "*". See text for a discussion of the various peaks. Product distributions in other DP clusters were similar. Abbreviations: Hex, hexose (+ 162 Da); Pen, pentose (+ 132 Da); ox, oxidized. **(D)** Illustration of the structure of a fragment of TXG (blue circle, glucose; orange star, xylose; yellow circle, galactose [43]; the position and number of galactosyl units vary) and possible cleavage sites for *Fg*LPMO9A (black arrows) and *Nc*LPMO9C (red arrows; see also ref. [21]).

Figure 4. Analysis of products generated from XG14^{OH}. (A) HPAEC-PAD chromatograms showing products generated upon incubation of XG14^{OH} with FgLPMO9A (blue line), as well as non-treated XG14^{OH} (black line) and the xyloglucan heptamer (XG7, XXXG) standard (orange line). (B) MALDI-ToF MS spectrum showing the sodium adduct of products generated from XG14^{OH} by FqLPMO9A (blue line) and the non-treated XG14^{OH} (black line); the indicated m/z values represent mass average. Numbers in parenthesis show $\Delta m/z$ compared to the mass of the native XG-oligosaccharide products, as explained in panel C; blue peaks are either from the substrate or the result of C1 oxidation which yields oxidized $(\Delta m/z = -2, "ox")$ and reduced $(\Delta m/z = +2, "red")$ oligomers; green peaks are the result of C4 oxidation $(\Delta m/z = 0$ for all species, hence no further indication of oxidation and reduction; see panel C). The peaks at m/z 1999.9, 2132.0 and higher represent the XG14^{OH} substrate (see black line), which contains a mixture of oligomers with varying degrees of galactosylation (see panel C). Reactions without ascorbic acid showed only these peaks. Due to high background signals in the lower mass range, the spectra are shown from m/z 800. (C) The substrate, XG14^{OH} (blue circle, glucose; orange star, xylose; yellow circle, galactose [43]), and comparison of the C1- and C4-oxidation products and their masses relative to the masses of native species. Parenthesis surrounding galactosyl-units signify that the number and position of these units vary. Abbreviations: Hex, hexose (+ 162.14 Da); Pen, pentose (+ 132.11 Da); red, reduced; ox, oxidized.



This article is protected by copyright. All rights reserved.

